

# Multi-level Reliable Guidance for Unpaired Multi-view Clustering

Like Xin, Wanqi Yang\*, Lei Wang, Ming Yang

**Abstract**—In this thesis, we address the challenging problem of unpaired multi-view clustering (UMC), which aims to achieve effective joint clustering using unpaired samples observed across multiple views. Traditional incomplete multi-view clustering (IMC) methods typically rely on paired samples to capture complementary information between views. However, such strategies become impractical in the UMC due to the absence of paired samples. Although some researchers have attempted to address this issue by preserving consistent cluster structures across views, effectively mining such consistency remains challenging when the cluster structures with low confidence. Therefore, we propose a novel method, Multi-level Reliable Guidance for UMC (MRG-UMC), which integrates multi-level clustering and reliable view guidance to learn consistent and confident cluster structures from three perspectives. Specifically, inner-view multi-level clustering exploits high-confidence sample pairs across different levels to reduce the impact of boundary samples, resulting in more confident cluster structures. Synthesized-view alignment leverages a synthesized-view to mitigate cross-view discrepancies and promote consistency. Cross-view guidance employs a reliable view guidance strategy to enhance the clustering confidence of poorly clustered views. These three modules are jointly optimized across multiple levels to achieve consistent and confident cluster structures. Furthermore, theoretical analyses verify the effectiveness of MRG-UMC in enhancing clustering confidence. Extensive experimental results show that MRG-UMC outperforms state-of-the-art UMC methods, achieving an average NMI improvement of 12.95% on multi-view datasets. The source code is available at: <https://anonymous.4open.science/r/MRG-UMC-5E20>.

**Index Terms**—Unpaired multi-view clustering, Multi-level clustering, Reliable view guidance, Confident cluster structure.

## I. INTRODUCTION

**D**ATA often exhibit diverse characteristics and representations, referred to as **multi-view data** [1]–[4]. In the real world, some instances lack data in one or more views, resulting in **incomplete multi-view data** [5], [6]. For example, in an image dataset, certain images may be missing specific visual or textual features. A more extreme yet realistic scenario arises when no paired observed samples exist between views [7], rendering the multi-view data as **unpaired multi-view data**. For example, in multi-camera surveillance systems, individual cameras may operate intermittently due to energy-saving or

maintenance, resulting in unpaired multi-view data [7]–[9]. Additionally, in a video, if we view a visible video and accompanying narrator text as separate views, the description may become disjointed from the visual content due to delays, resulting in the occurrence of unpaired multi-view data [10].

Clustering [11] serves as a potent technique for uncovering inherent patterns within data, segmenting samples into distinct clusters autonomously without supervised information. For the three types of datasets mentioned above, three downstream clustering tasks—multi-view clustering (**MC** [12]), incomplete multi-view clustering (**IMC** [13]), and unpaired multi-view clustering (**UMC** [8])—naturally emerge. Specifically, UMC is more challenging than MC and IMC due to the absence of paired samples. We summarize the differences between UMC and these general clustering methods (MC and IMC) from the following two perspectives. i) High practicality. Complete multi-view clustering assumes that all samples are observed across views, and incomplete multi-view clustering allows for partially observed samples. However, such ideal conditions are rarely met in real-world applications. For instance, in autonomous driving, LiDAR can detect distant vehicles, but cameras may miss them due to range limitations, making object association across views challenging. On different social platforms (e.g., X and LinkedIn), user data are not shared due to privacy concerns and business constraints, hindering personalized recommendations on emerging platforms. In finance, payment records from platforms such as Alipay, PayPal, and Apple Pay are mutually exclusive, as each transaction occurs only once on a specific platform, complicating fraud detection. Given these situations, UMC offers a more practical solution. ii) Independence from paired samples. Most complete and incomplete multi-view clustering methods rely on fully or partially paired samples to establish correspondences across views. In the absence of such correspondences, they often degenerate into independent single-view clustering, losing the ability to exploit cross-view complementarity. In contrast, our method assumes a consistent cluster structure across views, enabling the modeling of cross-view relationships without requiring paired samples, thereby offering greater flexibility and effectiveness for UMC.

Recently, some methods have leveraged consistent cluster structures to connect different views in UMC. For example, Yang *et al.* [7] leverage the covariance matrix to align different views. Xin *et al.* [8] use inner-view and cross-view contrastive learning to learn the consistent cluster structure. In addition, Xin *et al.* [9] leverage the view with the best clustering performance to align the other views. However, in UMC, learning consistent cluster structures across views

This work is supported by the National Natural Science Foundation of China (Nos. 62476136, 62276138), the Qing Lan Project of Jiangsu Province, China, and the Postgraduate Research & Practice Innovation Program of Jiangsu Province (KYCX24\_1865). Corresponding author: Wanqi Yang.

Like Xin is with the School of Mathematical Sciences, Nanjing Normal University, Nanjing, 210046, China. (e-mail: xinlike94@gmail.com).

Wanqi Yang and Ming Yang are with the School of Computer and Electronic Information, Nanjing Normal University, Nanjing, 210046, China. (e-mail: yangwq@njnu.edu.cn, myang@njnu.edu.cn).

Lei Wang is with the School of Computing and Information Technology, University of Wollongong, Australia. (e-mail: leiw@uow.edu.au).

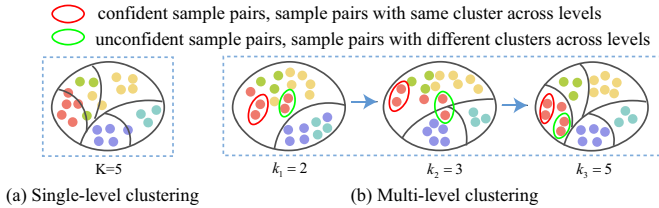


Fig. 1. The difference between single-level and multi-level clustering. In single-level clustering, some boundary samples typically emerge when there are  $K$  clusters. In contrast, multi-level clustering forms clusters progressively from a coarse set  $Cs = \{k_1, k_2, k_3\}$ . For the cluster  $k_3$ , high-confidence sample pairs are mined across different levels with the help of  $k_1$  and  $k_2$ , effectively reducing the number of boundary samples and resulting in a more confident cluster structure.

often overlooks issues such as noise, boundary samples and ambiguous clustering initialization, which may lead to cluster structures with low confident.

To address this issue, we propose *multi-level clustering to progressively enhance the quality of cluster structures at each level*, thereby achieving more confident cluster structures. Intuitively, coarse-grained classification is easier than fine-grained classification [14]. For example, distinguishing between two broad categories (*e.g.*, animals vs. plants) is much simpler than identifying finer categories (*e.g.*, flowers, trees, chickens, dogs, and horses). Similarly, coarse-grained clustering is less prone to errors than fine-grained clustering, and thus can serve as a helpful guide for the latter. As illustrated in Fig. 1 (a), clustering at a single-level may propagate boundary errors throughout the entire category, negatively impacting the final results. In contrast, Fig. 1 (b) demonstrates that multi-level clustering gradually organizes samples into coarse-to-fine groups, selectively leveraging confident sample pairs across different levels to reduce errors. This strategy ultimately yields a more stable and accurate cluster structure. Besides, it is worth noting that multi-level clustering in this thesis differs from hierarchical clustering. Hierarchical clustering follows a nested structure, where the clustering assignments of the next level are based on the previous ones. In contrast, multi-level clustering conducts clustering at each level separately and then selects high-confidence sample pairs across the different levels.

To learn a consistent and confidence cluster structure, we propose a novel method, MRG-UMC, consisting of three modules: i) Inner-view multi-level clustering: To address instability in cluster structures caused by boundary samples and ambiguous initial clustering, we use high-confidence sample pairs across different levels for each view to establish more confidence cluster structures. ii) Synthesized-view alignment: Direct alignment across views is challenging due to distribution discrepancies. At each level, a synthesized-view is introduced to assist in aligning other views, thereby enhancing consistency in cluster structures. iii) Cross-view guidance: Given the different clustering performances across views, the view with the best clustering result is selected as the reliable view to guide others at each level, resulting in more confident cluster structures. The main contributions are as follows:

- For the issue of learning consistent cluster structures with low confidence, we propose multi-level clustering and reliable view guidance to enhance clustering confidence.

- MRG-UMC is proposed to establish consistent and confident cluster structures across views, which comprises three modules: an inner-view multi-level clustering module, a synthesized-view alignment module, and a cross-view guidance module.
- Theoretical analyses validate the multi-level clustering and reliable view guidance in boosting the cluster structure confidence. Meanwhile, extensive results on five multi-view benchmark datasets demonstrate its superior performance.

## II. RELATED WORK

### A. Incomplete multi-view clustering

Recent advancements in clustering have focused on enhancing performance and extending applications across various domains. For instance, Bacciu *et al.* [15] proposed a mixture model for tree-structured data clustering. Kilic *et al.* [16] introduced a human-inspired method for feature selection. Additionally, clustering techniques have been successfully applied to biomonitoring [17].

However, in real-world scenarios, samples may be missing in one or more views due to various internal or external factors, resulting in incomplete multi-view data. To address this challenge in clustering tasks, researchers have extensively explored methods such as spectral approaches, subspace learning, and graph learning [7], [8]. In spectral approaches, Wen *et al.* [18] introduced a tensor spectral clustering method to recover missing views. Besides, they utilize latent information from absent views and capture intra-view data relationships often overlooked in other methods. Zhang *et al.* [19] restored latent connections between observed and unobserved samples, enhancing the robustness of subspace clustering through high-level correlations. It is the first attempt to formulate incomplete multi-view kernel subspace clustering from unified and tensorized perspectives. Wang *et al.* [20] used multiple kernel-based anchor graphs to tackle IMC, which adeptly captures both intra-view and inter-view nonlinear relationships by fusing multiple complete anchor graphs across views. To reduce the time required for recovering the original data, Zhang *et al.* [21] devised an approach that integrates spectral embedding completion and discrete cluster indicator learning into a unified step, providing a solution to this issue.

For graph learning, Li *et al.* [22] proposed the Joint Partition and Graph learning method, comprising two key components: unified partition space learning for noise robustness enhancement and consensus graph learning to uncover data structures. To explore the complex relationship between samples and latent representations, Zhu *et al.* [23] proposed a neighborhood constraint and a view-existence constraint for the first time. Moreover, in cases of arbitrary missing views, He *et al.* [24] proposed Structured Anchor-inferred Graph Learning. They replaced a fixed distance-based weighting matrix with a structural anchor-based similarity learning model, creating a trainable asymmetric intra-view similarity matrix. Additionally, to learn the overall optimal clustering result, Xia *et al.* [25] proposed a Kernelized Graph-based IMC algorithm, which optimizes downstream sub-tasks in a mutually reinforcing manner.

For subspace learning approaches, Yin *et al.* [26] devised a method for incomplete multi-view subspace learning, which enhances performance by simultaneously addressing feature selection and similarity preservation within and across views. To fully leverage observed samples, Yang *et al.* [27] employed a sparse and low-rank matrix to model correlations among samples within each view for imputing missing samples. They also enforce similar subspace representations to explore relationships between samples across different views, aiding clustering tasks. Due to the coefficient matrix, the self-representation method accurately captures sample relationships. Liu *et al.* [28] introduced a tailored self-representation subspace clustering algorithm for IMC, which integrates missing sample completion and self-representation learning into a cyclical process. Yang *et al.* [29] integrated the intrinsic consistency and extrinsic complementary information for prediction and cluster simultaneously. Li *et al.* [30] proposed a unified sparse subspace learning framework that integrates inter-view and intra-view affinities to generate a unified clustering assignment using a sparse anchor graph. However, obtaining paired samples across all views can be challenging in real-world scenarios.

### B. Unpaired multi-view clustering

UMC is an extreme scenario within IMC, where samples are solely observed in one view. This renders UMC more challenging compared to IMC [7], [8]. Numerous researchers have leveraged weak supervision information to establish correlations between views. For example, Qian *et al.* [31] and Houthuys *et al.* [32] integrated must-link and cannot-link constraints to build correlations across views in their studies. However, these approaches may prove ineffective without paired samples or supervised information.

For methods dealing with partially paired samples, Huang *et al.* [33] proposed Partially View-Aligned Clustering, which utilizes the ‘aligned’ data to learn a common space across different views and employs a neural network to establish category-level correspondence for unaligned data. Yang *et al.* [34] proposed Multiview Contrastive Learning with Noise-Robust Loss, which simultaneously learns representation and aligns data using a noise-robust contrastive loss. Furthermore, addressing both the partially view-unaligned and sample-missing problem, Yang *et al.* [35] introduced a more robust Multi-View Clustering method to directly re-align and recover samples from other views. Besides, Wang *et al.* [36] introduced the Cross-View Graph Contrastive Learning Network, which integrates multi-view information to align data and learn latent representations. Jin *et al.* [37] proposed a novel approach departing from traditional contrastive-based methods. They use pair-observed data alignment as ‘proxy supervised signals’ to guide instance-to-instance correspondences across views. Additionally, they introduce a prototype alignment module to rectify shifted prototypes in IMVC. Zhao *et al.* [38] learn soft clustering labels from complete data to capture category-level cross-view correspondences. However, these methods require some paired samples to establish relationships between views.

For methods dealing with unpaired data, Yang *et al.* [39] proposed the Noise-aware Image Captioning (NIC) method to make the most of trustworthy information in text with mismatched words. Specifically, NIC identified and explored mismatched words to reduce errors by assessing the reliability of word-label relationships based on inter-modal representativeness and intra-modal informativeness. Additionally, Yang *et al.* [7] introduced Iterative Multiview Subspace Learning for UMC to learn consistent subspace representations. Furthermore, they introduced another two methods to solve multi-view alignment and achieve end-to-end results, respectively. Besides, Xin *et al.* [8] proposed selective contrastive learning for UMC, leveraging inner-view and inter-view selective contrastive learning modules to improve cluster structure consistency. Furthermore, considering the differences in clustering performance across views, Xin *et al.* [9] leveraged the view with the best cluster performance to align the other views, thereby improving overall clustering performance. Although these methods explore consistent cluster structures across views, they cannot effectively mine consistency when the cluster structures are uncertain. Li *et al.* [40] address anchor and edge misalignments by proposing a Scalable Unpaired Multi-view Clustering with Bipartite Graph Matching. Notably, their definition of ‘unpaired’ refers to incorrect pairing relationships, whereas our work focuses on fully unpaired scenarios where no complete samples exist across any two views. That is the key distinction between them.

We compared our method with prior works in four aspects: i) Prior works does not consider unstable cluster structures, whereas MRG-UMC employs multi-level clustering to address this issue. ii) Regarding cross-view alignment, prior works aligns only views, while MRG-UMC also aligns clusters and samples through a synthesized-view module. iii) MRG-UMC provides theoretical support for multi-level clustering and reliable view guidance, whereas prior works lack such analysis. iv) Extensive experiments on multiple multi-view datasets demonstrate the superior performance of our approach compared to these methods.

### C. Dempster-Shafer evidence theory in multi-view learning

There have been several studies exploring confidence with Dempster-Shafer evidence theory. The theory was first proposed by Dempster and Shafer to deal with uncertainty based on belief functions [41]–[43]. Now, it has been developed a general framework. Recently, Han *et al.* [44] introduced multi-modal dynamics to enhance the reliability of fusion methods using evidence theory, dynamically evaluating feature-level and modality-level informativeness for dependable integration across diverse samples. Geng *et al.* [45] utilize uncertainty to weigh each view of individual samples based on data quality, maximizing the use of high-quality samples while minimizing the influence of noisy ones. Additionally, Han *et al.* [46] introduced a trusted multi-view classification method, dynamically integrating diverse views using the Dirichlet distribution for class probabilities and Dempster-Shafer theory for integration. Meanwhile, they also provide additional theoretical analysis to validate its effectiveness. For unreliable predictions in long-tailed classification, Li *et al.* [47] introduced the trustworthy

long-tailed classification method, which integrates classification and uncertainty estimation within a multi-expert framework, calculating evidence-based uncertainty and evidence for each expert, and merging these metrics using the Dempster-Shafer Evidence Theory.

#### D. Multi-level feature learning for multi-view clustering

For the method with multi-level feature learning, Xu *et al.* [48] proposed a method of multi-level feature learning with low-level features, high-level features, and semantic features to weaken the conflict between learning consistent semantics and inconsistent view-private information. To develop a robust network, Yang *et al.* [49] introduced the Cascade Deep Multi-Modal network structure with a cascade architecture, which maximizes correlations between layers sharing similar characteristics. Furthermore, Yang *et al.* [50] considered both user intentions and preferences, capturing users' dynamic information in hierarchical representations to solve the next-item recommendation. For the neglect of redundant information between views, Cui *et al.* [51] proposed a novel multi-view clustering framework based on information theory, utilizing the variational analysis to generate consistent information and enhance consistency through a sufficient representation of the lower bound. Besides, to tackle the issue of semantic consistency oversight in most methods, Zhou *et al.* [52] introduced a multi-level consistency collaborative learning framework, which learns cluster assignments of multiple views in the feature space and aligns semantic labels of different views through contrastive learning. Although these methods utilize multi-level representations or features to learn consistent information, they fail to account for the instability across different levels, which is a key distinction of our method.

### III. METHODOLOGY

#### A. Notations and Architecture

**Notations.** For the unpaired multi-view dataset  $\{\mathbf{X}^v\}_{v=1}^V$ , there are  $V$  views. The feature dimension of each view is denoted as  $d^v$ . For the  $v$ -th view, the number of samples is  $n^v$ . Therefore, the total number of samples in the unpaired multi-view dataset is  $N$ , where  $N = \sum_{v=1}^V n^v$ , since no paired samples exist in UMC. Specifically, in the  $v$ -th view, an autoencoder consists of an encoder  $F^v$  and a decoder  $G^v$ . We feed the  $v$ -th view data  $\mathbf{X}^v$  into the corresponding encoder  $F^v$  to learn the latent representation  $\mathbf{Z}^v$ , *i.e.*,  $\mathbf{Z}^v = F^v(\mathbf{X}^v)$ . In the inner-view multi-level clustering module, for sample  $\mathbf{z}_i^v$ , similarity sets for true positive pairs  $tp_{in}(\mathbf{z}_i^v)$  and the true negative pairs  $tn_{in}(\mathbf{z}_i^v)$  are constructed in the contrastive learning. In the synthesized-view alignment module, a matrix of cluster pairing relationships  $\mathbf{A}$  between views is established by the Hungarian Algorithm. Then, the similarity sets  $pos_{cro}(\mathbf{z}_i^v)$  and  $neg_{cro}(\mathbf{z}_i^v)$  for the positive and negative pairs of  $\mathbf{z}_i^v$  are constructed. In the cross-view guidance module, the silhouette coefficient  $sils^v$  is used to select reliable views. The set of reliable views  $\mathcal{R}$  includes those with a higher silhouette coefficient than the current view. Then we employ the KL divergence (*e.g.*,  $D(\mathbf{P}^r||\mathbf{Q}^v)$ ) to align the distribution  $\mathbf{Q}^v$  with  $\mathbf{P}^r$ , where  $\mathbf{P}^r$  and  $\mathbf{Q}^v$  denote approximate probability distributions of the  $r$ -th and  $v$ -th views. In the theoretical

analysis, as suggested by Dempster-Shafer Evidence Theory [46],  $\{b_k^r\}_{k=1}^K$  and  $\{b_k^o\}_{k=1}^K$  denote the belief masses from the reliable view and the original view, respectively.  $l$  represents the index of ground truth, while  $m$  denotes the index of the largest original belief mass in  $\{b_k^o\}_{k=1}^K$ .  $u^r$  and  $u^o$  represent the uncertainty masses for the reliable view and the original view, respectively, satisfying  $\sum_{k=1}^K b_k^r + u^r = 1$  and  $\sum_{k=1}^K b_k^o + u^o = 1$ . For clarification, the main symbols and their definitions are listed in the supplementary.

**The architecture of MRG-UMC.** We illustrate the training process with two views and five clusters. The cluster set  $Cs = \{k_1, k_2, k_3\}$  is defined as  $\{2, \lceil K/2 \rceil, K\}$ , where  $K$  is the true number of clusters, similar to [53]. As depicted in Fig. 2, the two-view samples  $(\mathbf{X}^1, \mathbf{X}^2)$  are fed into two autoencoders with regularization to learn view-specific subspace representations  $(\mathbf{Z}^1, \mathbf{Z}^2)$ . Subsequently, in the subspace, three modules are used to learn consistent and confident cluster structures. Initially, the clustering begins with  $k_1$  clusters, creating coarse-grained groupings. As training goes, the number of clusters increases to  $k_2$ , leading to finer-grained clusters. In the last stage, the cluster count is adjusted to  $k_3$ , resulting in a more refined cluster structure with the true number of clusters. For example, when the cluster number is  $k_3$ , in the inner-view multi-view clustering (indicated by the blue dashed box), a more confident cluster structure is established by leveraging confident sample pairs across three levels. In the synthesized-view alignment module (depicted in the green dashed box), each view aligns with the synthesized-view to reduce distribution discrepancies, thereby helping to learn consistent cluster structures. Furthermore, in the cross-view guidance module (shown in the red rectangular box), the reliable view guides the poorly clustered view to form a more confident cluster structure. After convergence, we perform  $K$ -means clustering on the concatenated matrix  $\mathbf{Z}^* = [\mathbf{Z}^1; \mathbf{Z}^2]$  to obtain the final clustering assignments.

**Multi-view autoencoders with regularizer.** Autoencoder [48] serves as a prevalent unsupervised model for projecting raw features into a latent feature space. Typically, an autoencoder includes an encoder and a decoder. For a given feature representation  $\mathbf{X}^v$  in the  $v$ -th view, we use an autoencoder to derive the latent representation  $\mathbf{Z}^v$  by minimizing the reconstruction loss. Additionally, to enhance the discriminative of  $\mathbf{Z}^v$ , we apply an orthogonal constraint to prevent it from expanding arbitrarily within the feature space [54] [55]. Therefore, for multi-view data, we obtain latent representations using autoencoders with a regularizer [7], [8] by:

$$l_{AE} = \sum_{v=1}^V \|\mathbf{X}^v - G^v(F^v(\mathbf{X}^v))\|_F^2 + \lambda_1 \|\mathbf{Z}^{vT} \mathbf{Z}^v - \mathbf{I}_d\|_F^2, \quad (1)$$

where  $F^v$  and  $G^v$  represent the encoder and decoder of the  $v$ -th autoencoder, respectively.  $\mathbf{Z}^v$  denotes the latent representation of  $\mathbf{X}^v$ .  $\lambda_1$  is a hyperparameter that adjusts the balance between the reconstruction term and the orthogonal constraint.

#### B. Methodology

**Multi-level clustering.** Due to the lack of supervision in clustering, cluster assignments can be uncertain, especially for

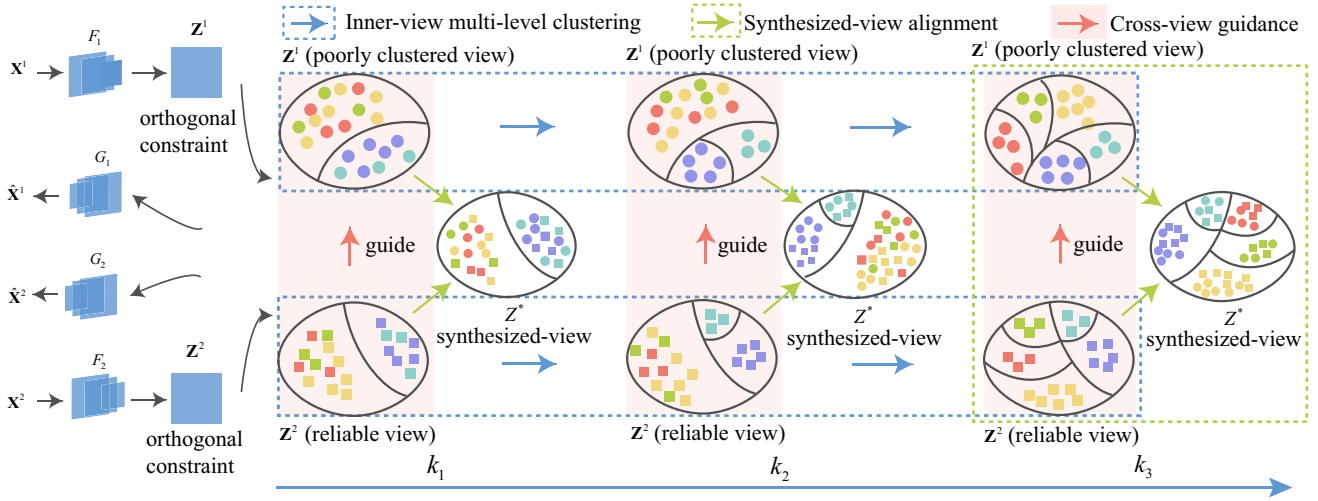


Fig. 2. The framework of Multi-level Reliable Guidance for UMC is built upon autoencoders with regularization. In latent spaces, training occurs in three stages with different numbers of clusters ( $k_1$ ,  $k_2$ , and  $k_3$ ). At each stage, three modules are employed: the inner-view multi-level clustering module, the synthesized-view alignment module, and the cross-view guidance module.

boundary samples. To mitigate the influence of such samples, various strategies have been proposed, including progressive sampling [56], [57] and adaptive weighting [58]–[60]. Typically, boundary samples are assigned small weights to reduce their influence. However, identifying boundary samples using a single-level approach may be unreliable. In addition, initial cluster assignments may be unstable due to limited training. To address these issues, we adopt a multi-level clustering strategy that categorizes samples progressively, thereby alleviating the negative effects of boundary samples and unstable initial assignments. Specifically, we draw on the concept of super-class [53], [61], [62] to construct the multi-level clustering. At each level, the method encourages samples to stay closer to the distribution of their corresponding super-class rather than those of others. Compared to direct pseudo-label assignment through single-level clustering, multi-level clustering offers softer results to ‘roughly categorize’ samples and reduces clustering errors step by step.

**Inner-view multi-level clustering.** In each view, samples can be grouped into clusters based on their distance from various cluster centroids. However, without supervised information, clustering assignments remain inherently uncertain. Contrastive learning is an unsupervised representation learning method that improves cluster performance by maximizing the similarities of positive pairs and minimizing the similarities of negative pairs in the feature space [48]. In clustering, the more accurately the relationships between samples are captured, the more confidence the cluster structures can be characterized. Therefore, to achieve confident cluster structures, instead of selecting high-confidence samples in contrastive learning, we leverage **high-confidence sample pairs**.

Following scl-UMC [8], we treat samples within the same cluster as positive pairs and those from different clusters as negative pairs. We then refine these pairings by classifying them into true and false categories based on the consistency of cluster relationships across multiple levels. For positive pairs, those that retain their positive correlation at each level are considered true positives, while those whose relationships vary across levels are labeled as false positives. Similarly, negative

pairs that consistently show negative correlations across levels are classified as true negatives, whereas pairs with inconsistent correlations are designated as false negatives.

Therefore, to enhance cluster structure confidence, high-confidence sample pairs, consisting of true positive and true negative examples, are employed in contrastive learning. To establish the correlation between samples, we first calculate the similarity between samples  $z_i^v$  and  $z_j^v$  using cosine similarity:

$$s_{ij}^v = \frac{z_i^v z_j^{v\top}}{\|z_i^v\| \cdot \|z_j^v\|}. \quad (2)$$

Similarly, we define the super-class set as [53], e.g.,  $C_s = \{k_1, k_2, k_3\}$ . Then, the similarities of true positive pairs  $tp_{in}(z_i^v)$  and true negative pairs  $tn_{in}(z_i^v)$  for  $z_i^v$  in the inner-view across three levels are designed as follows:

$$\begin{aligned} tp_{in}(z_i^v) &= \{s_{ij}^v : j = 1, 2, \dots, m_i^v, j \neq i, \\ &\quad ks(z_i^{v,k_1}) \cap ks(z_i^{v,k_2}) \cap ks(z_i^{v,k_3})\}, \\ tn_{in}(z_i^v) &= \{\widetilde{s}_{ij}^v : j = 1, 2, \dots, n_i^v, j \neq i, \\ &\quad kd(z_i^{v,k_1}) \cap kd(z_i^{v,k_2}) \cap kd(z_i^{v,k_3})\}, \end{aligned} \quad (3)$$

where  $m_i^v$  and  $n_i^v$  denote the number of true positive pairs and true negative pairs of  $z_i^v$ , respectively, intersecting across three different cluster levels.  $ks(z_i^{v,k_1})$  and  $kd(z_i^{v,k_1})$  denote the sets of samples with the same and different cluster assignments as  $z_i^v$  for  $k_1$  clusters, respectively. Similarly,  $ks(z_i^{v,k_2})$  and  $kd(z_i^{v,k_2})$  indicate the sets for  $k_2$  clusters, while  $ks(z_i^{v,k_3})$  and  $kd(z_i^{v,k_3})$  refer to the sets for  $k_3$  clusters.

With the assistance of high-confidence sample pairs, we then use the NT-Xent contrastive loss [63] across all views to learn the confident cluster structures across views as follows:

$$l_{in} = \frac{1}{V} \sum_{v=1}^V \sum_{i=1}^{n^v} \sum_{j=1}^{m_i^v} \frac{1}{n^v m_i^v} l_{ij}^v, \quad (4)$$

where

$$l_{ij}^v = -\log \frac{\exp(s_{ij}^v/\tau)}{\sum_{\widetilde{s}_{ij}^v \in tn_{in}(z_i^v)} \exp(\widetilde{s}_{ij}^v/\tau)}. \quad (5)$$

$n^v$  is the number of samples in the  $v$ -th view, and  $m_i^v$  represents the number of true positive pairs in the similarity set of  $\mathbf{z}_i^v$ , i.e.,  $m_i^v = |tp_{in}(\mathbf{z}_i^v)|$ . The set  $tn_{in}(\mathbf{z}_i^v)$  contains the true negative pairs of  $\mathbf{z}_i^v$ . Besides, the temperature parameter  $\tau$  is set to 0.1.

**Synthesized-view alignment.** Each view has its specific feature representation, making it challenging to directly align. To address this, we introduce a synthesized-view as an auxiliary view to reduce the discrepancy cross views. Specifically, the synthesized-view is constructed by concatenating multiple individual views, i.e.,  $\mathbf{Z}^* = [\mathbf{Z}^1; \dots; \mathbf{Z}^V]$ . Furthermore, to learn consistent cluster structures between views, we leverage contrastive learning to align each single view  $\{\mathbf{Z}^v\}_{v=1}^V$  with the synthesized-view  $\mathbf{Z}^*$ . However, without paired samples, it is challenging to explore the relationships between views. Therefore, we turn to establishing cluster pairing relationships and then aligning these clusters across views.

Firstly, we aim to construct the cluster pairing relationships between views. Specifically, we obtain the cluster centroids  $\mathbf{C}^*$  and  $\mathbf{C}^v$  from the synthesized-view and the  $v$ -th view using  $K$ -means clustering. Then, we calculate the weight matrix  $\mathbf{M}^v$  using  $\frac{\mathbf{C}^*(\mathbf{C}^v)^\top}{\|\mathbf{C}^*\| \cdot \|\mathbf{C}^v\|}$ . To acquire the pairing relationship, we transform the task of finding pairs of cluster centroids from two views into maximum-weight matching in a bipartite graph [64], [65]. The objective is to choose  $K$  entries from  $\mathbf{M}^v$ , where entries from each row and column maximize the overall weight matrix. Thus, learning the centroids pairing relationship becomes a maximum-weight matching issue, which can be solved by the Hungarian algorithm [66]. Naturally, the pairing relationship of cluster centroids  $\mathbf{A}^v$  between the synthesized-view  $\mathbf{Z}^*$  and the  $v$ -th view  $\mathbf{Z}^v$  is solved by the Hungarian Algorithm [8] as follows:

$$\begin{aligned} \max_{\mathbf{A}^v} \sum_{i=1}^K \sum_{j=1}^K m_{ij}^v a_{ij}^v, \\ \text{s.t. } \mathbf{A}^v \mathbf{A}^{v\top} = \mathbf{I}_K, \mathbf{A}^v \in \{0, 1\}^{K \times K} \end{aligned} \quad (6)$$

where  $m_{ij}^v \in \mathbf{M}^v$ ,  $a_{ij}^v \in \mathbf{A}^v$ . Then, the pairing correlation of clusters across views is obtained.

Secondly, we use contrastive learning to align pairing clusters. Specifically, in contrastive learning, positive sample pairs are samples with pairing clusters between a single view and the synthesized-view, while negative sample pairs are those with non-pairing clusters [8]. Similarly to Eq.(2), we calculate the similarity between  $\mathbf{z}_i^*$  and  $\mathbf{z}_j^v$  with cosine similarity  $s_{i,j}^{*v} = \mathbf{z}_i^* \mathbf{z}_j^{v\top} / (\|\mathbf{z}_i^*\| \cdot \|\mathbf{z}_j^v\|)$ . Then the positive similarity set  $pos_{cro}(\mathbf{z}_i^*)$  and negative similarity set  $neg_{cro}(\mathbf{z}_i^*)$  of  $\mathbf{z}_i^*$  are constructed as follows:

$$\begin{aligned} pos_{cro}(\mathbf{z}_i^*) &= \{s_{ij}^{*v} : v = 1, 2, \dots, V, j = 1, 2, \dots, n^v, a_{ij}^v = 1\}, \\ neg_{cro}(\mathbf{z}_i^*) &= \{\widetilde{s}_{ij}^{*v} : v = 1, 2, \dots, V, j = 1, 2, \dots, n^v, a_{ij}^v = 0\}, \end{aligned} \quad (7)$$

where  $s_{ij}^{*v}$  and  $\widetilde{s}_{ij}^{*v}$  are the similarities of  $\mathbf{z}_i^*$  and  $\mathbf{z}_j^v$  in positive pairs and negative pairs, respectively.  $a_{ij}^v = 1$  denotes that the cluster of  $\mathbf{z}_i^*$  in the synthesized-view matches the cluster of

$\mathbf{z}_j^v$  in the  $v$ -th view, and vice versa for  $a_{i,j}^v = 0$ . Therefore, the synthesized-view contrastive learning is formed as follows:

$$l_{sy} = \frac{1}{NV} \sum_{i=1}^N \sum_{v=1}^V \sum_{j=1}^{n^v} \frac{1}{n^v} l_{i,j}^{*v}, \quad (8)$$

where

$$l_{i,j}^{*v} = -\log \frac{\exp(s_{i,j}^{*v}/\tau)}{\sum_{\widetilde{s}_{i,j}^{*v} \in neg_{cro}} \exp(\widetilde{s}_{i,j}^{*v}/\tau)}. \quad (9)$$

$N$  and  $n^v$  represent the number of samples in the synthesized-view and the  $v$ -th view, respectively. The temperature parameter  $\tau$  is set to 0.1.

**Cross-view guidance.** Given the different clustering performances across views, we choose well-clustered views as reliable views to guide those with poor clustering performance. To assess the clustering quality of each view, we use the silhouette coefficient, which evaluates how well objects are grouped by comparing the distances within their cluster to those of other clusters [67]. In multi-view learning, the silhouette coefficient of the  $v$ -th view is defined as follows:

$$sil_s^v = \frac{1}{n^v} \sum_{i=1}^{n^v} sil(\mathbf{z}_i^v), \quad (10)$$

where  $sil(\mathbf{z}_i^v)$  is the silhouette coefficient of sample  $\mathbf{z}_i^v$  [67]. As for guidance, we employ the KL divergence [9] (e.g.,  $D(\mathbf{P}^r \parallel \mathbf{Q}^v)$ ), an asymmetric metric, to guide the distribution  $\mathbf{Q}^v$  with  $\mathbf{P}^r$ , where  $\mathbf{P}^r$  and  $\mathbf{Q}^v$  denote approximate probability distributions of the  $r$ -th (reliable view) and  $v$ -th view.

However, in the early stages of training, the clusters are not well-formed, leading to a low silhouette coefficient. Consequently, only the most reliable view is suitable for guiding the current views. As training goes on and the cluster structure becomes clearer, more views can be considered reliable for guiding the current view. To capture this process, we use a decreasing coefficient  $\tau$  to dynamically select reliable views. Specifically, the initial coefficient  $\tau$  is set to 1.5 and decreases by 0.99 each epoch until it reaches 1. For each view, the set of reliable views is defined as those with a silhouette coefficient greater than  $\tau$  times that of the current view, denoted as  $\mathcal{R}$ . Consequently, the loss for the cross-view guidance module is formulated as follows:

$$l_{cr} = \sum_{v=1}^V \sum_{r=1}^{|\mathcal{R}|} \frac{1}{V^2} \mathbf{P}^r \log\left(\frac{\mathbf{P}^r}{\mathbf{Q}^v}\right), \quad (11)$$

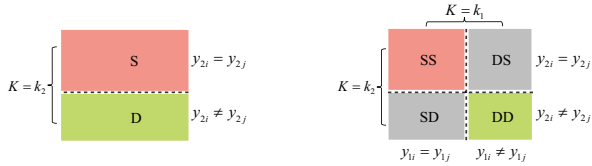
where the indices of the reliable view and the current view are denoted by  $r$  and  $v$ , respectively.  $|\mathcal{R}|$  represents the number of reliable views for the  $v$ -th view.

In summary, MRG-UMC is formulated to capture consistent and confident cluster structures as follows:

$$L = l_{AE} + \lambda_2 l_{in} + \lambda_3 l_{sy} + \lambda_4 l_{cr}, \quad (12)$$

where  $l_{AE}$ ,  $l_{in}$ ,  $l_{sy}$  and  $l_{cr}$  are the terms of an autoencoder network with orthogonal constraint, inner-view multi-level clustering, synthesized-view alignment, and cross-view guidance, respectively. Besides,  $\lambda_2$ ,  $\lambda_3$ , and  $\lambda_4$  are the hyperparameters to balance these terms.

**Algorithm and convergence analysis.** The algorithm for MRG-UMC and the training loss curves for four datasets



(a) High-level clustering with  $k_2$  clusters (b) Multi-level clustering with  $k_1$  and  $k_2$  clusters

Fig. 3. The Venn diagram illustrates the sample sets in high-level and multi-level clustering, where  $k_1 < k_2$ . ‘S’ denotes the similar set, and ‘D’ denotes the dissimilar set.

are provided in the supplementary. We further analyze the convergence. Each term in Eq. (12) is non-negative. Hence, the total objective function is bounded below by zero, *i.e.*,  $L \geq 0$ . In addition,  $\mathcal{L}$  is smooth and differentiable almost everywhere. During training, we employ the Adam optimizer with a fixed learning rate of 0.0001, a mini-batch size of 256, and default hyperparameters. According to theoretical results in [68], Adam converges to a first-order stationary point under the following mild conditions:

- The objective function is smooth and bounded below;
- The variance of the stochastic gradients is finite;
- The learning rate is sufficiently small and constant.

Under these conditions, the training loss is almost surely guaranteed to converge to a local minimum *i.e.*,  $\lim_{t \rightarrow \infty} \mathbb{E} [\|\nabla \mathcal{L}(\theta_t)\|^2] = 0$ . More detailed theoretical discussions are provided in the supplementary material.

In our experiments, we empirically define convergence as the point at which the relative change in loss,  $|L_t - L_{t-1}|/L_{t-1}$ , remains below  $1 \times 10^{-4}$  for 10 consecutive epochs, within a maximum of 200 epochs. As shown in Figure 1 (supplementary), our model consistently satisfies this criterion across all datasets. These empirical results, along with the satisfaction of the above theoretical conditions, support the convergence of our method.

### C. Theory Analysis

To enhance the confidence of cluster structure, we employ two strategies: multi-level clustering and reliable view guidance. Then, we theoretically validate the effectiveness of these strategies and arrive at the following conclusions: i) Multi-level clustering helps reduce inconsistencies across different levels, thereby improving the confidence of cluster structures. ii) Guidance from a reliable view can potentially enhance the belief masses of poorly clustered views, thereby increasing the confidence in these views.

**Proposition 1.** *Given a dataset  $\mathbf{X}$ , assuming it initially yields a low-level cluster assignment  $\mathbf{Y}_1$  with  $k_1$  clusters, followed by a high-level cluster assignment  $\mathbf{Y}_2$  with  $k_2$  clusters ( $k_1 < k_2$ ). Then four sets of samples are generated based on the cluster assignments:*

$$\begin{aligned}
 SS &= \{(x_i, x_j) | y_{1i} = y_{1j}, y_{2i} = y_{2j}, i \neq j\}, \\
 DD &= \{(x_i, x_j) | y_{1i} \neq y_{1j}, y_{2i} \neq y_{2j}, i \neq j\}, \\
 SD &= \{(x_i, x_j) | y_{1i} = y_{1j}, y_{2i} \neq y_{2j}, i \neq j\}, \\
 DS &= \{(x_i, x_j) | y_{1i} \neq y_{1j}, y_{2i} = y_{2j}, i \neq j\}.
 \end{aligned} \tag{13}$$

*In multi-level clustering with high-level and low-level clusters, removing sample sets (SD and DS) with inconsistent relationships between the two levels reduces cluster structure*

*inconsistency, thereby improving the confidence in the cluster structure.*

As shown in Fig. 3 (a), samples are directly divided into a similarity set (S) and a dissimilarity set (D) in high-level clustering with  $k_2$  clusters. However, clustering errors are inevitable. In Fig. 3 (b), in high-level clustering with cluster assignment  $\mathbf{Y}_2$ , removing sample sets  $SD$  with different cluster relationships in  $\mathbf{Y}_1$  would reduce cluster structure inconsistency and enhance the confidence of the high-level cluster structure. Besides, the  $DS$  set contains few samples, and even if they exist, they are likely boundary samples. Removing the  $DS$  set will certainly reduce clustering inconsistency. Therefore, multi-level clustering is better than single-level clustering for learning the confident cluster structure.

**Proposition 2.** *Based on Dempster-Shafer Evidence Theory [46], [69], guidance from reliable views enhances the belief mass in the original view. That is, for the  $l$ -th class (the ground-truth class), under the condition that the belief mass of the reliable view ( $b_l^r$ ) is not lower than any belief mass from the original view ( $\{b_k^o\}_{k=1}^K$ ), the reliable view can enhance the belief mass of the original view ( $b_l \geq b_l^o$ ). Here,  $b_l^r$  and  $b_l$  represent the belief masses of the original view for the ground-truth class before and after integrating the reliable view, respectively.*

**Proof.**

$$\begin{aligned}
 b_l &= \frac{b_l^o b_l^r + b_l^o u^r + b_l^r u^o}{\sum_{k=1}^K b_k^o b_k^r + u^o + u^r - u^o u^r} \quad // \text{Eq.(13) in [46]} \\
 &\geq \frac{b_l^o (b_l^r + u^r + u^o)}{b_m^o (1 - u^r) + u^o + u^r - u^o u^r} \quad // b_l^r \geq b_l^o \\
 &\geq \frac{b_l^o (b_l^r + u^r + u^o)}{b_m^o + u^r + u^o} \quad // \text{Removing } (-b_m^o u^r - u^o u^r) \\
 &\geq b_l^o. \quad // b_l^r \geq b_m^o
 \end{aligned} \tag{14}$$

where  $b_m^o$  denotes the largest original belief mass in the set  $\{b_k^o\}_{k=1}^K$ . Therefore, for the  $l$ -class, if the belief mass  $b_l^r$  on the reliable view exceeds any value in the original set of belief masses  $\{b_k^o\}_{k=1}^K$ , integrating  $b_l^r$  from the reliable view can potentially enhance the belief mass  $b_l^o$  of the original view, thereby increasing confidence in the cluster structure. A more detailed analysis is provided in the supplementary material.

Clustering is inherently unsupervised and sensitive to boundary samples and initialization, often resulting in cluster structures with low confidence. To address this, our theoretical analysis is designed to enhance confidence in clustering structures. Besides, these two propositions have wide applicability. Specifically, Proposition 1 supports a more confident cluster structure by reducing the influence of boundary samples, which is crucial for improving stability in applications such as autonomous driving and medical diagnostics. Proposition 2 demonstrates that leveraging reliable views to guide others can significantly improve the belief mass of the other view, especially in real-world settings like cross-modal healthcare analysis and financial fraud detection.

## IV. TESTS

In this section, we conduct a series of tests to evaluate the effectiveness of MRG-UMC, including comparative experiments, verification experiments for two key propositions,

TABLE I  
COMPARISON OF RELATED MULTI-VIEW CLUSTERING METHODS ON MULTI-VIEW DATASETS. THE SYMBOL ‘-’ INDICATES OUT OF MEMORY.

Methods	Digit (6views)			Scene-15 (3views)			Caltech101-20 (6views)			Flower17 (7views)			Reuters (5views)		
	NMI	ACC	F1	NMI	ACC	F1	NMI	ACC	F1	NMI	ACC	F1	NMI	ACC	F1
OPMC (ICCV2021)	12.31	18.33	17.42	17.23	18.94	14.01	12.42	14.30	14.69	13.52	13.38	10.14	11.11	19.48	20.41
OP-LFMVC (ICML2021)	22.54	11.57	19.90	9.73	17.02	11.02	13.38	17.34	13.56	9.71	14.88	8.02	-	-	-
DAU-Nets (AAAI2021)	17.10	19.40	16.82	22.62	21.52	16.30	24.50	15.34	17.90	14.84	13.81	10.77	2.20	25.06	22.98
RMVC (AAAI2018)	22.31	26.25	17.88	28.84	24.68	18.03	21.72	18.90	17.34	19.08	17.28	11.24	-	-	-
DSMVC (CVPR2022)	13.95	16.50	7.80	19.86	19.38	10.09	19.44	14.71	2.60	13.55	12.50	4.57	1.53	19.06	15.12
AWMVC (AAAI2023)	12.72	18.65	14.79	20.95	22.08	15.08	22.32	17.23	18.10	14.17	13.68	9.04	2.57	23.44	24.01
UOMvSC (TKDE2023)	15.51	18.85	18.17	26.59	24.55	16.75	24.48	16.64	17.50	14.70	13.09	10.99	-	-	-
WMVEC-FP (KBS2024)	10.75	18.25	16.24	7.34	31.56	26.23	17.19	19.04	12.09	1.92	6.62	10.89	3.77	28.37	32.78
CVCL (ICCV2023)	67.35	61.70	55.69	38.37	33.33	31.88	48.86	31.82	24.35	45.64	44.58	38.39	-	-	-
DAIMC (IJCAI2018)	18.17	25.68	17.96	12.49	19.46	18.68	12.49	19.46	18.68	8.56	12.75	9.83	-	-	-
UEAF (AAAI2019)	10.32	19.25	16.63	11.59	15.65	12.56	9.28	27.03	24.26	3.91	7.54	10.74	-	-	-
IMSC-AGL (TCYB2020)	24.01	17.61	17.38	16.45	20.88	12.99	17.30	15.81	12.97	12.66	14.93	8.69	-	-	-
OPMC (Bigdata2017)	12.02	20.03	16.70	11.53	16.09	11.74	18.29	19.26	17.31	12.68	14.68	9.13	-	-	-
OPIMC (AAAI2019)	20.13	27.74	19.66	15.48	20.33	13.35	17.10	20.18	16.71	11.76	16.39	8.87	10.92	27.46	26.13
FCMVC (TIP2024)	12.39	22.55	14.91	9.32	17.15	10.17	9.73	13.29	10.28	8.05	14.59	7.46	5.46	24.93	21.74
T-UMC (TCYB2022)	9.09	17.70	15.06	26.51	27.65	22.91	11.95	14.08	9.01	11.66	15.74	13.57	-	-	-
GIGA (PR2024)	8.84	17.50	18.95	15.45	16.48	15.67	21.16	16.26	13.03	15.73	15.00	15.40	-	-	-
UPMGC-SM (AAAI2024)	31.43	35.36	28.47	21.35	26.04	16.50	16.84	16.49	10.58	26.20	24.65	16.91	-	-	-
IUMC-CA (TNNLS2023)	75.16	54.53	60.82	<u>50.25</u>	34.98	34.47	58.31	33.42	33.24	<b>66.13</b>	48.52	44.19	-	-	-
IUMC-CY (TNNLS2023)	74.64	60.72	61.17	<b>56.75</b>	30.58	35.34	61.48	46.63	<b>45.06</b>	63.23	49.21	40.19	10.07	22.99	21.48
scl-UMC (TNNLS2023)	72.75	60.00	50.97	49.62	39.15	33.51	59.63	57.94	60.93	<u>65.65</u>	49.93	47.80	30.73	52.83	31.32
RG-UMC (TNNLS2024)	77.37	84.85	84.65	49.23	<u>53.82</u>	<u>49.82</u>	65.81	67.05	38.92	58.57	50.04	47.81	30.93	<b>59.78</b>	<u>34.54</u>
RGs-UMC (TNNLS2024)	86.19	92.83	92.77	47.40	53.50	48.11	70.88	75.28	41.50	60.64	52.02	51.68	32.26	57.24	33.35
MRG-UMC	<b>88.36</b>	<b>93.99</b>	<b>93.92</b>	49.42	<b>53.88</b>	<b>50.47</b>	<b>72.82</b>	<b>76.48</b>	<u>42.01</u>	61.76	<b>54.85</b>	<b>53.33</b>	<b>40.71</b>	<u>58.29</u>	<b>37.47</b>

ablation studies, visualization and so on. Besides, the hyperparameter analysis is provided in the supplementary material.

**Datasets.** The five benchmark multi-view datasets (*Digit*<sup>1</sup>, *Scene-15*<sup>2</sup>, *Caltech101-20*<sup>2</sup>, *Flower17*<sup>3</sup>, and *Reuters*<sup>4</sup>) used in this paper are the same as those in [8]. To simulate the unpaired multi-view scenario, samples from each view of these multi-view datasets are randomly selected at a ratio of  $1/V$  ( $V$  is the number of views), ensuring no paired samples between views. Specifically, to maintain class balance,  $1/V$  of the samples from each class are selected in each view, forming the unpaired multi-view data.

**Comparison methods.** Among the 28 state-of-the-art comparison methods, we include 9 complete MC methods (OPMC [70], OP-LFMVC [71], DUA-Nets [45], RMVC [72], DSMVC [73], AWMVC [74], UOMvSC [75], WMVEC-FP [76] and CVCL [77]), 11 IMC methods (DAIMC [78], UEAF [79], IMSC-AGL [80], OMVC [81], OPIMC [82], MvCLN [34], Completer [13], FCMVC [83], T-UMC [67], GIGA [84], and ICMVC [85]), and 8 UMC methods (UPMGC-SM [10], IUMC-CA [7], IUMC-CY [7], MGCCFF [38], SURE [35], scl-UMC [8], RG-UMC [9], and RGs-UMC [9]). All complete and incomplete multi-view learning methods adopt mean imputation to handle missing data, consistent with their original experimental settings. Moreover, all comparative methods are implemented using open-source code with the optimal parameters recommended in their respective papers.

**Implementation details.** MRG-MUC is implemented in PyTorch 1.13, and all evaluations run on a standard Ubuntu 20.04

OS with NVIDIA 2080Ti GPU. The network architecture used in our work follows that of [8], [13], with each layer including a batch normalization layer and a ReLU layer. For training, we set the maximum number of epochs to 200 and employed mini-batch gradient descent with a batch size of 256. We used the Adam optimizer with default parameters to train our model, and the learning rate is set to 0.0001. Specifically, the cluster set  $C_s$  is  $\{2, \lceil K/2 \rceil, K\}$  for all datasets, as in [53], where  $K$  denotes the true number of clusters. Once the training process converges, all unpaired samples are passed through the autoencoder network with the saved parameters to obtain the latent feature representations  $\{Z^v\}_{v=1}^V$ . We then obtain the final clustering result by applying  $K$ -means clustering to the concatenated representation  $Z = [Z^1; Z^2; \dots; Z^V]$ . We use accuracy (ACC), Normalized Mutual Information (NMI), and F1-score (F1) as evaluation metrics and report the average results from 10 runs.

#### A. Performance Comparison and Analysis

**Clustering performance comparison of methods on multi-view datasets.** We compared our model with 23 methods across five multi-view datasets, excluding MvCLN [34], Completer [13], ICMVC [85], MGCCFF [38], and SURE [35], which are specifically designed for two-view settings. From TABLE I, we observe the following:

i) Our method surpasses all MC and IMC methods, demonstrating its superior effectiveness in UMC over the MC and IMC approaches. Typically, MC and IMC methods rely on paired samples between views for clustering. However, when handling unpaired multi-view data, missing information must be recovered, as noted in [83], which is inherently prone to errors. Fortunately, our method constructs relationships between views through pairing clusters, avoiding recovery errors.

<sup>1</sup><http://archive.ics.uci.edu/dataset/72/multiple+features>

<sup>2</sup><https://github.com/XLearning-SCU/2021-CVPR-Completer/tree/main/data>

<sup>3</sup><http://www.robots.ox.ac.uk/vgg/data/flowers/17/index.html>

<sup>4</sup><http://archive.ics.uci.edu/ml/datasets/Reuters+RCV1+RCV2+Multilingual%2C+Multiview+Text+Categorization+Test+collection>

TABLE II  
COMPARISON OF RELATED MULTI-VIEW CLUSTERING METHODS FOR UMC ON TWO VIEWS DATASETS.

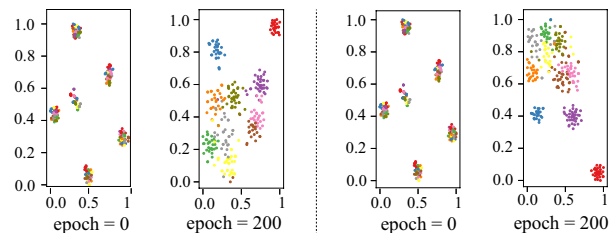
Methods	<i>Digit</i>			<i>Scene-15</i>			<i>Caltech101-20</i>			<i>Flower17</i>			<i>Reuters</i>		
	<i>NMI</i>	<i>ACC</i>	<i>F1</i>	<i>NMI</i>	<i>ACC</i>	<i>F1</i>	<i>NMI</i>	<i>ACC</i>	<i>F1</i>	<i>NMI</i>	<i>ACC</i>	<i>F1</i>	<i>NMI</i>	<i>ACC</i>	<i>F1</i>
<b>OPMC</b> (ICCV2021)	44.12	51.75	32.02	30.43	27.29	19.76	27.59	28.12	24.71	26.19	24.56	14.91	20.17	40.32	36.73
<b>OP-LFMVC</b> (ICML2021)	39.04	46.40	35.10	15.60	20.45	13.28	21.61	22.09	17.46	20.81	23.31	13.09	-	-	-
<b>DUA-Nets</b> (AAAI2021)	42.08	38.07	33.98	30.12	27.80	21.23	32.40	29.26	25.42	28.34	24.44	18.61	4.28	26.23	24.17
<b>RMVC</b> (AAAI2018)	46.75	44.05	36.56	36.34	30.52	21.92	34.37	24.43	22.11	33.70	28.24	18.83	-	-	-
<b>DSMVC</b> (CVPR2022)	49.84	41.90	8.39	27.00	25.22	6.03	32.14	22.34	5.29	26.69	23.46	4.14	10.86	30.39	14.40
<b>AWMVC</b> (AAAI2023)	41.45	44.05	31.76	30.39	28.63	20.17	33.11	33.74	29.24	27.76	26.19	16.31	24.43	36.70	35.01
<b>UOMvSc</b> (TKDE2023)	52.56	41.95	37.09	34.81	30.01	21.99	35.18	26.45	22.72	29.28	26.18	16.43	-	-	-
<b>WMVEC-FP</b> (KBS2024)	37.55	41.75	22.12	27.31	30.68	22.97	21.37	21.56	12.96	13.35	13.01	10.07	11.98	31.09	30.92
<b>CVCL</b> (ICCV2023)	69.07	73.70	73.32	38.41	33.06	29.65	47.75	39.07	26.79	31.84	32.16	30.63	-	-	-
<b>DAIMC</b> (IJCAI2018)	39.37	38.50	30.88	19.46	22.79	16.20	20.16	24.81	22.88	21.87	21.03	15.12	-	-	-
<b>UEAF</b> (AAAI2019)	30.90	26.77	19.32	22.16	20.14	13.19	25.44	22.19	32.54	12.72	9.25	6.37	-	-	-
<b>IMSC-AGL</b> (TCYB2020)	48.99	45.40	37.09	27.61	27.98	18.33	30.04	24.06	20.38	26.99	24.71	15.31	-	-	-
<b>OMVC</b> (BigData2017)	31.69	34.87	20.64	0.68	9.16	12.94	26.11	26.78	22.62	26.08	24.52	14.47	-	-	-
<b>OPIMC</b> (AAAI2019)	41.49	44.60	37.01	20.32	23.52	15.30	22.38	24.48	21.97	19.90	21.84	12.22	8.99	27.53	24.36
<b>MvCLN</b> (CVPR2021)	41.96	45.10	52.41	21.50	21.43	22.47	31.21	28.04	17.64	19.57	17.65	18.43	20.18	18.97	19.72
<b>Completer</b> (CVPR2021)	41.35	39.66	40.24	23.24	21.86	19.59	34.29	26.37	22.61	22.65	20.73	19.83	1.28	23.84	19.67
<b>FCMVC</b> (TIP2024)	37.31	45.65	32.55	17.21	23.63	13.40	24.55	21.04	17.47	14.91	18.16	9.96	11.75	39.12	27.73
<b>T-UMC</b> (TCYB2022)	46.15	49.85	49.26	40.75	39.20	30.10	38.84	35.88	23.54	22.44	22.65	16.51	-	-	-
<b>GIGA</b> (PR2024)	52.17	40.45	41.62	13.25	14.72	12.84	47.73	33.49	26.30	24.67	20.96	20.53	-	-	-
<b>ICMVC</b> (AAAI2024)	25.54	30.20	30.39	12.62	18.02	17.67	33.86	21.46	17.31	35.49	27.72	26.98	13.84	35.60	26.00
<b>UPMGC-SM</b> (TNNLS2024)	39.41	38.46	28.99	25.42	24.38	14.72	23.38	20.88	19.25	23.60	23.72	14.09	-	-	-
<b>IUMC-CA</b> (TNNLS2023)	46.20	27.75	29.82	40.50	30.08	27.39	35.91	26.40	19.24	<b>43.31</b>	31.84	25.64	-	-	-
<b>IUMC-CY</b> (TNNLS2023)	49.17	45.55	37.72	39.67	18.68	23.87	32.22	28.08	35.06	39.52	18.82	21.01	11.34	27.50	27.36
<b>scl-UMC</b> (TNNLS2023)	57.00	60.85	61.35	45.26	36.59	35.35	38.60	41.52	36.84	39.98	32.21	35.06	39.50	49.86	41.12
<b>MGCCFF</b> (AAAI2025)	65.66	68.79	60.41	36.79	34.59	25.97	60.75	43.66	48.28	29.21	27.53	19.25	-	-	-
<b>SURE</b> (TPAMI2022)	64.93	52.05	54.18	48.03	36.68	36.50	64.82	43.04	32.34	25.77	24.34	23.79	53.59	45.88	42.42
<b>RG-UMC</b> (TNNLS2024)	92.38	96.40	96.42	46.79	49.53	47.40	<b>78.64</b>	<b>73.89</b>	<b>55.46</b>	42.01	<u>43.75</u>	<u>42.80</u>	53.56	60.53	39.13
<b>RGs-UMC</b> (TNNLS2024)	<u>93.93</u>	<u>97.20</u>	<u>97.21</u>	<b>48.57</b>	<u>52.19</u>	<u>50.70</u>	<u>76.37</u>	71.17	54.50	41.35	41.62	42.30	<u>55.82</u>	<b>71.96</b>	<u>56.18</u>
<b>MRG-UMC</b>	<b>94.11</b>	<b>97.30</b>	<b>97.31</b>	<u>47.90</u>	<b>53.86</b>	<b>51.22</b>	76.19	<u>71.52</u>	<u>54.58</u>	<u>42.66</u>	<b>43.75</b>	<b>42.83</b>	<b>56.62</b>	<u>63.43</u>	<b>56.40</b>

ii) Compared with six state-of-the-art UMC methods, our model achieves average improvements of 12.95%, 14.99%, and 11.62% in NMI, ACC, and F-score, respectively, indicating a positive effect on clustering performance. Specifically, MRG-UMC achieves an average improvement of 3.14% in NMI, 1.32% in ACC, and 1.96% in F-score compared to RGs-UMC, highlighting the effectiveness of our method in learning confident cluster structures. In contrast, RGs-UMC fails to account for the confidence in cluster structures across views, resulting in inferior results.

**Clustering performance comparison of methods on two-view datasets.** Following [13], we evaluate our method on two-view datasets. For the five datasets, *Digit* and *Flower17* use their first two views as two-view datasets, while the remaining datasets follow the settings from [8], [13]. TABLE II summarizes the results against 27 methods, leading to the following observations: (i) Compared with MC and IMC methods, MRG-UMC consistently outperforms all of them, demonstrating superior effectiveness in UMC. (ii) MRG-UMC also surpasses the other UMC methods, achieving average improvements of 15.56% in NMI, 18.23% in ACC, and 18.69% in F-score. These improvements are attributed to the multi-level clustering mechanism, which reduces clustering errors, as well as the modules designed to enhance the learning of consistent and confident cluster structures.

### B. Validation of Two Propositions

To evaluate the impact of multi-level clustering described in Proposition 1, we conducted two experimental analyses.



(a) Clustering with single-level clustering (b) Clustering with multi-level clustering  
Fig. 4. Evolution of the latent representation on the *Digit* dataset (6 views and 10 clusters) for Proposition 1. Each color denotes a cluster.

**(1) The performance between single-level and multi-level clustering.** To validate Proposition 1, we compare single-level clustering and multi-level clustering on four datasets. The results from Table III show that multi-level clustering performance outperforms its single-level counterpart, confirming the effectiveness of proposition 1. Specifically, on four datasets, multi-level clustering achieves an average improvement of 2.66%, 2.34%, and 2.61% over single-level clustering in terms of NMI, ACC, and F1, respectively.

**(2) Visualization the clustering between single-level and multi-level clustering.** To further demonstrate the effectiveness of multi-level clustering, we visualize the clustering evolution on the latent representations of the *Digit* dataset with six views, as shown in Fig. 4. By comparing Fig. 4(a) and Fig. 4(b), we observe that multi-level clustering improves sample separability and compactness, with fewer samples incorrectly merged near decision boundaries, which is consistent with the analysis of Proposition 1 in Fig. 3.

TABLE III  
COMPARE SINGLE-LEVEL AND MULTI-LEVEL CLUSTERING OF MRG-UMC ON FOUR DATASETS WITH MULTIPLE VIEWS.

Strategy	Digit (6views)			Scene-15 (3views)			Caltech101-20 (6views)			Flower17 (7views)		
	NMI	ACC	F1	NMI	ACC	F1	NMI	ACC	F1	NMI	ACC	F1
single-level clustering	86.60	92.93	92.86	44.34	49.07	45.86	71.05	75.32	38.62	59.72	52.52	51.95
multi-level clustering	88.36	93.99	93.92	49.42	53.88	50.47	72.82	76.48	42.01	61.76	54.85	53.33

TABLE IV  
PERFORMANCE OF MRG-UMC WITH AND WITHOUT RELIABLE VIEW GUIDANCE ON FOUR DATASETS.

Strategy	Digit (6views)			Scene-15 (3views)			Caltech101-20 (6views)			Flower17 (7views)		
	NMI	ACC	F1	NMI	ACC	F1	NMI	ACC	F1	NMI	ACC	F1
w/o reliable view guidance	17.44	22.58	23.39	19.05	18.96	17.46	44.34	49.07	45.86	15.89	14.82	13.30
with reliable view guidance	88.36	93.99	93.92	49.42	53.88	50.47	72.82	76.48	42.01	61.76	54.85	53.33

TABLE V  
THE CLUSTERING PERFORMANCE OF EACH VIEW WITH AND WITHOUT RELIABLE VIEW GUIDANCE

View	Digit (6views)			Caltech101-20 (6views)		
	NMI	ACC	F1	NMI	ACC	F1
W/o reliable view guidance						
V1	42.95	47.58	46.70	32.21	31.62	19.68
V2	70.42	66.97	64.07	39.19	38.30	21.04
V3	47.23	57.88	55.61	33.46	40.87	19.74
V4	65.29	59.70	58.20	57.82	55.01	23.62
V5	53.82	58.18	56.80	46.40	36.25	20.02
V6	66.76	63.03	59.73	44.24	39.33	18.62
With reliable view guidance						
V1	88.07	88.79	88.29	66.95	58.35	39.76
V2	97.63	98.79	98.79	61.76	46.79	34.33
V3	93.50	96.36	96.23	65.53	48.59	34.11
V4	97.05	98.48	98.48	66.18	47.04	32.32
V5	89.84	84.55	82.35	70.73	64.78	40.58
V6	75.31	76.67	72.03	70.83	60.93	43.25

To validate the effectiveness of reliable view guidance as described in Proposition 2, we conducted three experimental analyses.

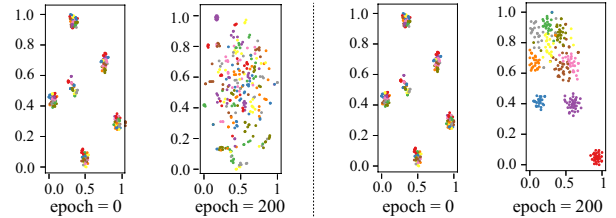
(1) **Performance of reliable view guidance.** We evaluate the clustering performance with and without reliable view guidance, as shown in Table IV. From the results in Table IV, we can clearly observe the significant impact of reliable view guidance.

(2) **Individual view performance under reliable view guidance.** Furthermore, we examine the impact of reliable view guidance on each individual view, with detailed results presented in Table V. The results demonstrate that reliable view guidance effectively enhances clustering performance at the view level.

(3) **Visualization of clustering under reliable view guidance.** To further illustrate the effectiveness of reliable view guidance (*i.e.*, cross-view) guidance, we visualize the clustering evolution in Fig. 5. Comparing panels (a) and (b), we observe that in the absence of cross-view guidance, the clustering structure becomes noticeably less coherent. Furthermore, comparing Fig. 4 with Fig. 5, the results suggest that cross-view guidance contributes more significantly than multi-level clustering to the formation of well-structured clusters.

### C. Ablation Study and Visualization

**Ablation study of MRG-UMC.** To further analyze the modules in MRG-UMC, we conducted ablation studies on four datasets (*Digit*, *Scene-15*, *Caltech101-20* and *Flower17*).



(a) Clustering without reliable view guidance (b) Clustering with reliable view guidance  
Fig. 5. Evolution of the latent representation on the *Digit* dataset (6 views and 10 clusters) for Proposition 2. Each color denotes a cluster.

Specifically, we evaluated different combinations of the orthogonal constraint (*Orth*), the inner-view multi-level clustering (*In*), the synthesized-view alignment module (*Sy*), and the cross-view guidance module (*Cr*). The results of the ablation studies are presented in TABLE VI.

As observed from TABLE VI, the combination of all modules performs the best (Line 12), which is our method MRG-UMC. In detail, when comparing Lines 2-5 with Line 1, it is evident that the *Cr* module has the most significant impact on clustering, validating the importance of reliable view guidance. Subsequently, the following ablations are based on the *Cr* module. Taking the *Digit* dataset as an example, when comparing Lines 6-8 with Line 5, it is evident that the *Orth* module and *Sy* module are more effective than the *In* module in learning the cluster structure. The *Orth* module aids in learning discriminative features, while the *Sy* module facilitates to alignment of different views. Besides, the *In* module helps to progressively merge confident cluster structures through multi-level clustering. Moreover, comparing Lines 9-11 with Lines 6-8 shows that these three modules complement each other and improve performance. The same conclusion can be drawn from other datasets in TABLE VI.

**Single-view performance.** MRG-UMC utilizes a consistent cluster structure to connect different views. To validate the effectiveness of MRG-UMC on each view, we evaluate its performance across three datasets and compare it with three other methods, as shown in Fig. 6. i) Comparing the *K*-means clustering method with all the other methods validates the effectiveness of exploring a consistent cluster structure. ii) Comparing scl-UMC and RG-UMC with MRG-UMC, we observed significant improvements in clustering performance for each view. This shows that a more confident cluster structure helps to improve clustering performance.

**Visualization.** To show the effectiveness of learning consistent cluster structures and achieving alignment, we use t-SNE to track the evolution every 20 epochs during training on the

TABLE VI  
ABLATION ANALYSIS OF MRG-UMC CONDUCTED ON FOUR DATASETS.

Line	Orth	In	Co	Cr	Digit (6views)			Scene-15 (3views)			Caltech101-20 (6views)			Flower17 (7views)		
					NMI	ACC	F1	NMI	ACC	F1	NMI	ACC	F1	NMI	ACC	F1
1					15.12	20.86	21.19	20.81	20.28	18.44	19.40	23.69	12.57	15.45	13.98	14.20
2	✓				15.23	21.67	22.36	21.40	21.02	19.27	20.48	27.59	13.33	13.48	13.14	13.47
3		✓			15.07	22.07	23.04	21.01	20.37	18.64	18.10	41.39	12.21	11.75	11.61	11.76
4			✓		14.88	21.52	21.92	21.15	21.00	20.44	23.35	21.81	13.86	14.73	14.06	13.10
5				✓	83.04	90.45	90.35	41.44	47.41	42.87	64.14	64.82	34.27	38.95	36.90	36.00
6	✓			✓	85.27	92.07	91.99	42.06	47.84	44.96	70.02	67.35	36.75	56.04	48.66	45.67
7		✓		✓	85.30	92.22	92.12	42.02	46.97	45.73	67.68	65.21	36.51	43.12	38.81	34.42
8			✓	✓	85.44	92.22	92.14	41.48	46.83	43.03	70.42	74.29	38.64	47.52	43.54	40.45
9	✓	✓		✓	85.57	92.47	92.41	43.01	48.11	44.11	70.74	75.49	38.90	55.94	50.50	48.79
10	✓		✓	✓	85.47	92.22	92.13	42.41	50.93	48.13	69.26	70.69	38.21	54.63	49.81	47.00
11		✓	✓	✓	85.84	92.22	92.10	41.09	49.27	45.70	70.78	73.35	39.98	47.57	45.30	43.72
12	✓	✓	✓	✓	<b>88.36</b>	<b>93.99</b>	<b>93.92</b>	<b>46.09</b>	<b>53.08</b>	<b>50.47</b>	<b>72.82</b>	<b>76.48</b>	<b>42.01</b>	<b>61.76</b>	<b>54.85</b>	<b>53.33</b>

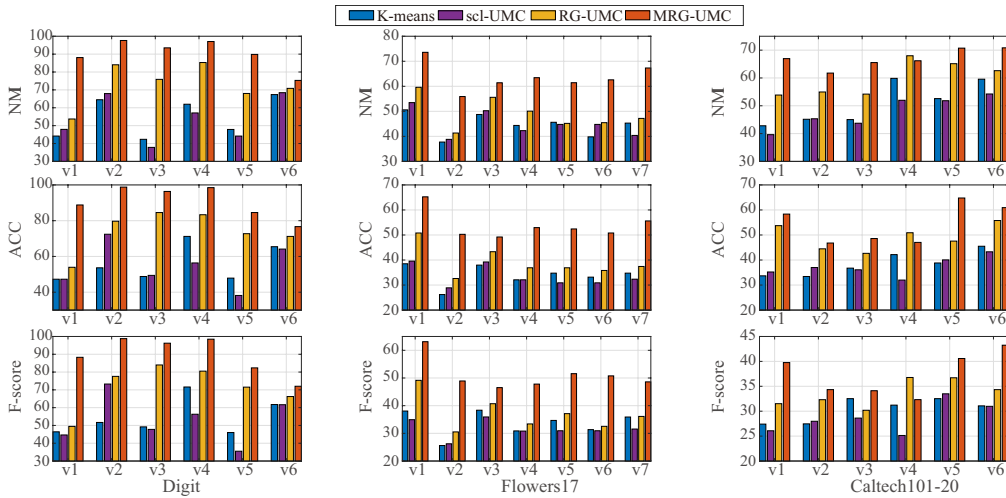


Fig. 6. The single-view performance of three comparison methods across three datasets.

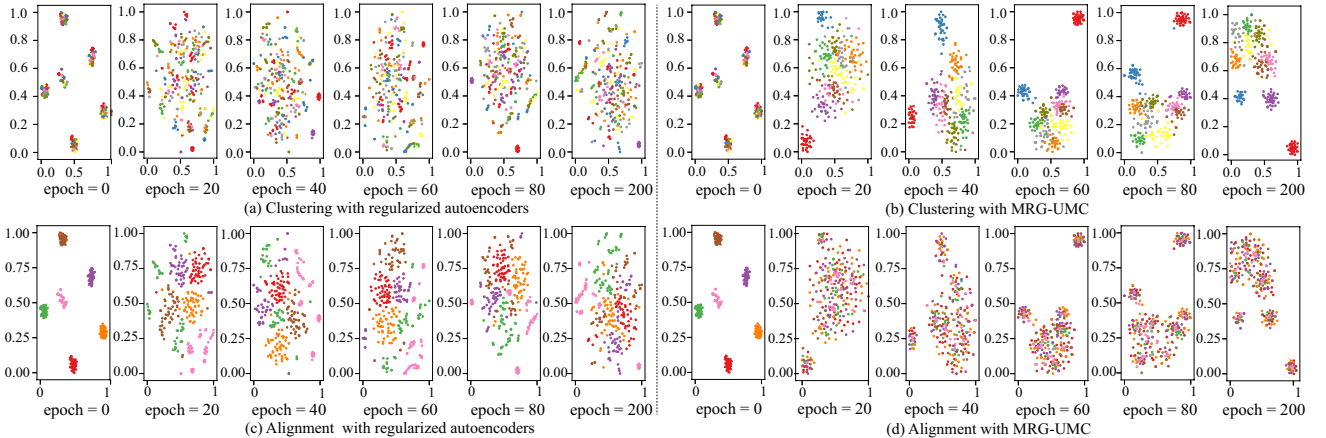


Fig. 7. Comparison of visualizations between MRG-UMC and the MRG-UMC model with only regularized autoencoders. The evolution of latent representations on the *Digit* dataset with ten clusters and six views during the training process. In the first and second rows, colors represent clusters and views, respectively.

*Digit* dataset with multiple views. For clarity, we randomly sample 500 samples and visualize the evolution in Fig. 7. In Fig. 7 (a-b), colors represent cluster assignments predicted by  $K$ -means, while in Fig. 7 (c-d), colors indicate different views. Specifically, to highlight the effectiveness of our method, we compare the visualizations of MRG-UMC (Fig. 7 (b) and (d)) with those of the MRG-UMC model with only regularized autoencoders (*i.e.*, Eq. (1)) (Fig. 7 (a) and (c)).

From Fig. 7, we observe: i) Comparing Fig. 7 (a) and (b), the three modules of MRG-UMC aid in forming cluster structures.

Similarly, comparing Fig. 7 (c) and (d), MRG-UMC efficiently and quickly aligns different views. ii) From Fig. 7 (b), we see that initially, features are mixed, with most samples grouped into a few clusters. As training progresses, cluster assignments improve, and features become more distinct. This demonstrates the effectiveness of MRG-UMC in learning clear cluster structures. iii) Fig. 7 (d) shows that our method successfully aligns samples from different views. Initially, the samples are separated by view, but as training goes on, they quickly come into alignment.

TABLE VII  
FLOPS AND TOTAL PARAMETER OF MRG-UMC ON FOUR DATASETS  
WITH MULTIPLE VIEWS

Datasets	<i>Digit</i> (6views)	<i>Scene15</i> (3views)	<i>Caltech101-20</i> (6views)	<i>Flower17</i> (7views)
Total params (MB)	4.63	4.52	4.57	7.26
GFLOPs	1.18	1.15	1.17	1.36

TABLE VIII  
EXTERNAL INDICATORS EVALUATION ON TWO DATASETS

Methods	<i>Digit (6views)</i>					<i>Caltech101-20 (6views)</i>				
	NMI	ACC	sil $\uparrow$	DB $\downarrow$	CHI $\uparrow$	NMI	ACC	sil $\uparrow$	DB $\downarrow$	CHI $\uparrow$
WMVEC-FP	10.75	18.25	-0.07	<u>2.93</u>	34.94	17.19	19.04	<b>0.62</b>	<u>2.42</u>	<b>85.95</b>
FCMVC	12.39	22.55	-0.45	17.89	33.33	9.73	13.29	-0.26	13.03	5.83
GIGA	8.84	17.50	<u>0.10</u>	5.85	11.35	21.16	16.26	-0.01	5.26	10.02
UPMGC-SM	31.43	35.36	-0.30	20.66	34.52	16.84	16.49	-0.69	16.60	15.62
RG-UMC	77.37	84.85	0.03	4.79	42.09	65.81	67.05	0.07	5.16	26.04
RGs-UMC	<u>86.19</u>	<u>92.83</u>	0.04	4.19	<u>43.52</u>	<u>70.88</u>	<u>75.28</u>	0.09	5.03	30.74
MRG-UMC	<b>88.36</b>	<b>93.99</b>	<b>0.15</b>	<b>2.53</b>	<b>192.48</b>	<b>72.82</b>	<b>76.48</b>	<u>0.19</u>	<b>2.41</b>	<b>86.31</b>

**Complexity analysis.** We analyze the computational complexity of MRG-UMC by computing the number of parameters and floating-point operations (FLOPs) [86], [87] across four datasets in Table VII. Across the four datasets, MRG-UMC maintains a total parameter size below 10 MB and requires less than 1.5 GFLOPs, highlighting its efficiency and suitability for scalable or real-time clustering applications.

**Cluster evaluation validity index.** To evaluate the effectiveness of MRG-UMC in terms of clustering quality, we compare it with six state-of-the-art methods published in 2024 using three widely adopted internal metrics: Silhouette Coefficient (sil) [67], Davies-Bouldin Index (DB), and Calinski-Harabasz Index (CHI) [88]. The Silhouette Coefficient ranges from  $[-1, 1]$ , with higher values indicating a better clustering structure. The DB Index ranges from 0 to  $+\infty$ , where lower values are preferred. The CHI Index also ranges from 0 to  $+\infty$ , with higher values indicating better cluster compactness and separation. Experiments are conducted on two representative unpaired multi-view datasets, *Digit* and *Caltech101-20*, with results summarized in Table VIII. As shown, MRG-UMC consistently outperforms other methods across most metrics, demonstrating more semantically meaningful clustering with improved intra-cluster compactness and inter-cluster separability. In contrast, some methods (e.g., WMVEC-FP) yield high internal scores (sil, DB, and CHI) and exhibit clear cluster structures, yet perform poorly on external metrics (NMI and ACC), suggesting a misalignment between the learned clusters and the ground truth labels.

## V. CONCLUSION AND FUTURE WORK

Mining consistency among views is challenging when the cluster structures with low confidence. To address this issue, we propose a novel method called Multi-level Reliable Guidance for UMC (MRG-UMC) to enhance the confidence of cluster structures. Specifically, MRG-UMC consists of three modules: inner-view multi-level clustering, synthesized-view alignment, and cross-view guidance. Ultimately, our method demonstrates outstanding performance in UMC, as evidenced by both theoretical analysis and extensive test results.

In future work, we plan to enhance the robustness of multi-view models. For the ever-changing reality, ensuring the reliability, security, and cleanliness of data becomes increasingly challenging. Furthermore, while many methods aim to enhance overall performance, they often neglect weaker performance on individual views. Consequently, we will further investigate algorithms within stable and secure frameworks.

## REFERENCES

- [1] C. Xu, D. Tao, and C. Xu, "A survey on multi-view learning," *arXiv preprint arXiv:1304.5634*, 2013.
- [2] W. Yang, Y. Gao, Y. Shi, and L. Cao, "Mrm-lasso: A sparse multiview feature selection method via low-rank analysis," *IEEE transactions on neural networks and learning systems*, vol. 26, no. 11, pp. 2801–2815, 2015.
- [3] Y. Yang, H. Wei, H. Zhu, D. Yu, H. Xiong, and J. Yang, "Exploiting cross-modal prediction and relation consistency for semisupervised image captioning," *IEEE Transactions on Cybernetics*, vol. 54, no. 2, pp. 890–902, 2024.
- [4] Y. Yang, J. Yang, R. Bao, D. Zhan, H. Zhu, X. Gao, H. Xiong, and J. Yang, "Corporate relative valuation using heterogeneous multi-modal graph neural network," *IEEE Transactions on Knowledge and Data Engineering*, vol. 35, no. 1, pp. 211–224, 2021.
- [5] C. Xu, D. Tao, and C. Xu, "Multi-view learning with incomplete views," *IEEE Transactions on Image Processing*, vol. 24, no. 12, pp. 5812–5825, 2015.
- [6] Y. Yang, D. Zhan, X. Sheng, and Y. Jiang, "Semi-supervised multi-modal learning with incomplete modalities," in *IJCAI*, 2018, pp. 2998–3004.
- [7] W. Yang, L. Xin, L. Wang, M. Yang, W. Yan, and Y. Gao, "Iterative multiview subspace learning for unpaired multiview clustering," *IEEE Transactions on Neural Networks and Learning Systems*, vol. 35, no. 10, pp. 14 848–14 862, 2024.
- [8] L. Xin, W. Yang, L. Wang, and M. Yang, "Selective contrastive learning for unpaired multi-view clustering," *IEEE Transactions on Neural Networks and Learning Systems*, vol. 36, no. 1, pp. 1749–1763, 2025.
- [9] L. Xin, W. Yang, L. Wang, and M. Yang, "Unpaired multiview clustering via reliable view guidance," *IEEE Transactions on Neural Networks and Learning Systems*, vol. 36, no. 6, pp. 11 443–11 455, 2025.
- [10] Y. Wen, S. Wang, Q. Liao, W. Liang, K. Liang, X. Wan, and X. Liu, "Unpaired multi-view graph clustering with cross-view structure matching," *IEEE Transactions on Neural Networks and Learning Systems*, vol. 35, no. 11, pp. 16 049–16 063, 2024.
- [11] Y. Yang and H. Wang, "Multi-view clustering: A survey," *Big Data Mining and Analytics*, vol. 1, no. 2, pp. 83–107, 2018.
- [12] U. Fang, M. Li, J. Li, L. Gao, T. Jia, and Y. Zhang, "A comprehensive survey on multi-view clustering," *IEEE Transactions on Knowledge and Data Engineering*, vol. 35, no. 12, pp. 12 350–12 368, 2023.
- [13] Y. Lin, Y. Gou, Z. Liu, B. Li, J. Lv, and X. Peng, "Completer: Incomplete multi-view clustering via contrastive prediction," in *Proceedings of the IEEE/CVF conference on computer vision and pattern recognition*, 2021, pp. 11 174–11 183.
- [14] N. Sohoni, J. Dunnmon, G. Angus, A. Gu, and C. Ré, "No subclass left behind: Fine-grained robustness in coarse-grained classification problems," *Advances in Neural Information Processing Systems*, vol. 33, pp. 19 339–19 352, 2020.
- [15] D. Bacciu and D. Castellana, "Bayesian mixtures of hidden tree markov models for structured data clustering," *Neurocomputing*, vol. 342, pp. 49–59, 2019.
- [16] U. Kilić, E. S. Essiz, and M. K. Keles, "Binary anarchic society optimization for feature selection," *Romanian Journal of Information Science and Technology*, vol. 26, no. 3–4, pp. 351–364, 2023.
- [17] G. Duka, S. Travin, I. Zinicovscaia, and R.-E. Precup, "Approach to evaluate the data of moss biomonitoring studies: Preprocessing and preliminary ranking," *Romanian Journal of Information Science and Technology*, vol. 26, pp. 276–288, 2023.
- [18] J. Wen, Z. Zhang, Z. Zhang, L. Zhu, L. Fei, B. Zhang, and Y. Xu, "Unified tensor framework for incomplete multi-view clustering and missing-view inferring," in *Proceedings of the AAAI conference on artificial intelligence*, vol. 35, no. 11, 2021, pp. 10 273–10 281.
- [19] G. Zhang, D. Huang, and C. Wang, "Unified and tensorized incomplete multi-view kernel subspace clustering," *IEEE Transactions on Emerging Topics in Computational Intelligence*, vol. 8, no. 2, pp. 1550–1566, 2024.

- [20] S. Wang, J. Cao, F. Lei, J. Jiang, Q. Dai, and B. W. Ling, "Multiple kernel-based anchor graph coupled low-rank tensor learning for incomplete multi-view clustering," *Applied Intelligence*, vol. 53, no. 4, pp. 3687–3712, 2023.
- [21] C. Zhang, J. Wei, B. Wang, Z. Li, C. Chen, and H. Li, "Robust spectral embedding completion based incomplete multi-view clustering," in *Proceedings of the 31st ACM International Conference on Multimedia*, 2023, pp. 300–308.
- [22] L. Li, Z. Wan, and H. He, "Incomplete multi-view clustering with joint partition and graph learning," *IEEE Transactions on Knowledge and Data Engineering*, vol. 35, no. 1, pp. 589–602, 2023.
- [23] P. Zhu, X. Yao, Y. Wang, M. Cao, B. Hui, S. Zhao, and Q. Hu, "Latent heterogeneous graph network for incomplete multi-view learning," *IEEE Transactions on Multimedia*, vol. 25, pp. 3033–3045, 2023.
- [24] W. He, Z. Zhang, Y. Chen, and J. Wen, "Structured anchor-inferred graph learning for universal incomplete multi-view clustering," *World Wide Web*, vol. 26, no. 1, pp. 375–399, 2023.
- [25] D. Xia, Y. Yang, S. Yang, and T. Li, "Incomplete multi-view clustering via kernelized graph learning," *Information Sciences*, vol. 625, pp. 1–19, 2023.
- [26] Q. Yin, S. Wu, and L. Wang, "Unified subspace learning for incomplete and unlabeled multi-view data," *Pattern Recognition*, vol. 67, no. 67, pp. 313–327, 2017.
- [27] W. Yang, Y. Shi, Y. Gao, L. Wang, and M. Yang, "Incomplete-data oriented multiview dimension reduction via sparse low-rank representation," *IEEE Transactions on Neural Networks and Learning Systems*, vol. 29, no. 12, pp. 6276–6291, 2018.
- [28] J. Liu, X. Liu, Y. Zhang, P. Zhang, W. Tu, S. Wang, S. Zhou, W. Liang, S. Wang, and Y. Yang, "Self-representation subspace clustering for incomplete multi-view data," in *Proceedings of the 29th ACM international conference on multimedia*, 2021, pp. 2726–2734.
- [29] Y. Yang, D. Zhan, Y. Wu, Z. Liu, H. Xiong, and Y. Jiang, "Semi-supervised multi-modal clustering and classification with incomplete modalities," *IEEE Transactions on Knowledge and Data Engineering*, vol. 33, no. 2, pp. 682–695, 2019.
- [30] A. Li, C. Feng, Z. Wang, Y. Sun, Z. Wang, and L. Sun, "Anchor-based sparse subspace incomplete multi-view clustering," *Wireless Networks*, vol. 30, no. 6, pp. 5559–5570, 2024.
- [31] Q. Qian, S. Chen, and X. Zhou, "Multi-view classification with cross-view must-link and cannot-link side information," *Knowledge-Based Systems*, vol. 54, no. 4, pp. 137–146, 2013.
- [32] L. Houthuys and J. A. K. Suykens, "Unpaired multi-view kernel spectral clustering," in *2017 IEEE Symposium Series on Computational Intelligence (SSCI)*, 2017, pp. 1–7.
- [33] Z. Huang, P. Hu, J. T. Zhou, J. Lv, and X. Peng, "Partially view-aligned clustering," *Advances in Neural Information Processing Systems*, vol. 33, pp. 2892–2902, 2020.
- [34] M. Yang, Y. Li, Z. Huang, Z. Liu, P. Hu, and X. Peng, "Partially view-aligned representation learning with noise-robust contrastive loss," in *Proceedings of the IEEE/CVF conference on computer vision and pattern recognition (CVPR)*, June 2021, pp. 1134–1143.
- [35] M. Yang, Y. Li, P. Hu, J. Bai, J. Lv, and X. Peng, "Robust multi-view clustering with incomplete information," *IEEE Transactions on Pattern Analysis and Machine Intelligence*, vol. 45, no. 1, pp. 1055–1069, 2022.
- [36] Y. Wang, D. Chang, Z. Fu, J. Wen, and Y. Zhao, "Partially view-aligned representation learning via cross-view graph contrastive network," *IEEE Transactions on Circuits and Systems for Video Technology*, vol. 34, no. 8, pp. 7272–7283, 2024.
- [37] J. Jin, S. Wang, Z. Dong, X. Liu, and E. Zhu, "Deep incomplete multi-view clustering with cross-view partial sample and prototype alignment," in *Proceedings of the IEEE/CVF conference on computer vision and pattern recognition*, 2023, pp. 11 600–11 609.
- [38] L. Zhao, Z. Wang, X. Wang, Z. Chen, and B. Xu, "Incomplete and unpaired multi-view graph clustering with cross-view feature fusion," in *Proceedings of the AAAI Conference on Artificial Intelligence*, vol. 39, no. 21, 2025, pp. 22 786–22 794.
- [39] P. Zeng, M. Yang, Y. Lu, C. Zhang, P. Hu, and X. Peng, "Semantic invariant multi-view clustering with fully incomplete information," *IEEE Transactions on Pattern Analysis and Machine Intelligence*, vol. 46, no. 4, pp. 2139–2150, 2023.
- [40] X. Li, Y. Pan, Y. Sun, Y. Sun, Q. Sun, Z. Ren, and I. W. Tsang, "Scalable unpaired multi-view clustering with bipartite graph matching," *Information Fusion*, vol. 116, p. 102786, 2025.
- [41] A. P. Dempster, "Upper and lower probabilities induced by a multivalued mapping," in *Classic works of the Dempster-Shafer theory of belief functions*. Springer, 2008, pp. 57–72.
- [42] G. Shafer, *A mathematical theory of evidence*. Princeton university press, 1976, vol. 42.
- [43] A. P. Dempster, "A generalization of bayesian inference," *Journal of the Royal Statistical Society: Series B (Methodological)*, vol. 30, no. 2, pp. 205–232, 1968.
- [44] Z. Han, F. Yang, J. Huang, C. Zhang, and J. Yao, "Multimodal dynamics: Dynamical fusion for trustworthy multimodal classification," in *Proceedings of the IEEE/CVF conference on computer vision and pattern recognition*, 2022, pp. 20 707–20 717.
- [45] Y. Geng, Z. Han, C. Zhang, and Q. Hu, "Uncertainty-aware multi-view representation learning," in *Proceedings of the AAAI Conference on Artificial Intelligence*, vol. 35, no. 9, 2021, pp. 7545–7553.
- [46] Z. Han, C. Zhang, H. Fu, and J. T. Zhou, "Trusted multi-view classification with dynamic evidential fusion," *IEEE transactions on pattern analysis and machine intelligence*, vol. 45, no. 2, pp. 2551–2566, 2022.
- [47] B. Li, Z. Han, H. Li, H. Fu, and C. Zhang, "Trustworthy long-tailed classification," in *Proceedings of the IEEE/CVF Conference on Computer Vision and Pattern Recognition*, 2022, pp. 6970–6979.
- [48] J. Xu, H. Tang, Y. Ren, L. Peng, X. Zhu, and L. He, "Multi-level feature learning for contrastive multi-view clustering," in *Proceedings of the IEEE/CVF Conference on Computer Vision and Pattern Recognition*, 2022, pp. 16 051–16 060.
- [49] Y. Yang, Y. Wu, D. Zhan, and Y. Jiang, "Deep multi-modal learning with cascade consensus," in *PRICAI 2018: Trends in Artificial Intelligence: 15th Pacific Rim International Conference on Artificial Intelligence, Nanjing, China, August 28–31, 2018, Proceedings, Part II 15*. Springer, 2018, pp. 64–72.
- [50] N. Zhu, J. Cao, Y. Liu, Y. Yang, H. Ying, and H. Xiong, "Sequential modeling of hierarchical user intention and preference for next-item recommendation," in *Proceedings of the 13th international conference on web search and data mining*, 2020, pp. 807–815.
- [51] C. Cui, Y. Ren, J. Pu, J. Li, X. Pu, T. Wu, Y. Shi, and L. He, "A novel approach for effective multi-view clustering with information-theoretic perspective," *Advances in neural information processing systems*, vol. 36, pp. 44 847–44 859, 2023.
- [52] Y. Zhou, Q. Zheng, Y. Wang, W. Yan, P. Shi, and J. Zhu, "Mcoco: Multi-level consistency collaborative multi-view clustering," *Expert Systems with Applications*, vol. 238, p. 121976, 2024.
- [53] G. Gui, Z. Zhao, L. Qi, L. Zhou, L. Wang, and Y. Shi, "Improving barely supervised learning by discriminating unlabeled samples with super-class," *Advances in Neural Information Processing Systems*, vol. 35, pp. 19 849–19 860, 2022.
- [54] M. Chen, T. Liu, C. Wang, D. Huang, and J. Lai, "Adaptively-weighted integral space for fast multiview clustering," in *Proceedings of the 30th ACM International Conference on Multimedia*, 2022, pp. 3774–3782.
- [55] M. Chen, C. Wang, D. Huang, J. Lai, and P. S. Yu, "Efficient orthogonal multi-view subspace clustering," in *Proceedings of the 28th ACM SIGKDD Conference on Knowledge Discovery and Data Mining*, 2022, pp. 127–135.
- [56] Y. Yang, Y. Zhang, X. Song, and Y. Xu, "Not all out-of-distribution data are harmful to open-set active learning," *Advances in Neural Information Processing Systems*, vol. 36, pp. 13 802–13 818, 2023.
- [57] Y. Yang, N. Jiang, Y. Xu, and D. Zhan, "Robust semi-supervised learning by wisely leveraging open-set data," *IEEE Transactions on Pattern Analysis and Machine Intelligence*, vol. 46, no. 12, pp. 8334–8347, 2024.
- [58] J. Shen, Y. Zhang, H. Liang, Z. Zhao, K. Zhu, K. Qian, Q. Dong, X. Zhang, and B. Hu, "Depression recognition from eeg signals using an adaptive channel fusion method via improved focal loss," *IEEE Journal of Biomedical and Health Informatics*, vol. 27, no. 7, pp. 3234–3245, 2023.
- [59] Z. Liu, H. Huang, and S. Letchmunan, "Adaptive weighted multi-view evidential clustering," in *International Conference on Artificial Neural Networks*. Springer, 2023, pp. 265–277.
- [60] R. He, Z. Han, Y. Yang, and Y. Yin, "Not all parameters should be treated equally: Deep safe semi-supervised learning under class distribution mismatch," in *Proceedings of the AAAI Conference on Artificial Intelligence*, vol. 36, no. 6, 2022, pp. 6874–6883.
- [61] B. Zhang, Y. Wang, W. Hou, H. Wu, J. Wang, M. Okumura, and T. Shinzaki, "Flexmatch: Boosting semi-supervised learning with curriculum pseudo labeling," *Advances in Neural Information Processing Systems*, vol. 34, pp. 18 408–18 419, 2021.
- [62] K. Sohn, D. Berthelot, N. Carlini, Z. Zhang, H. Zhang, C. A. Raffel, E. D. Cubuk, A. Kurakin, and C. Li, "Fixmatch: Simplifying semi-supervised learning with consistency and confidence," *Advances in neural information processing systems*, vol. 33, pp. 596–608, 2020.

- [63] T. Chen, S. Kornblith, M. Norouzi, and G. Hinton, "A simple framework for contrastive learning of visual representations," in *International conference on machine learning*. PMLR, 2020, pp. 1597–1607.
- [64] A. Grinman, "The hungarian algorithm for weighted bipartite graphs," *Massachusetts Institute of Technology*, 2015.
- [65] D. Bruff, "The assignment problem and the hungarian method," *Notes for Math*, vol. 20, no. 29-47, p. 5, 2005.
- [66] M. Wright, "Speeding up the hungarian algorithm," *Computers and Operations Research*, vol. 17, no. 1, pp. 95–96, 1990.
- [67] J. Lin, M. Chen, C. Wang, and H. Zhang, "A tensor approach for uncoupled multiview clustering," *IEEE Transactions on Cybernetics*, vol. 54, no. 2, pp. 1236–1249, 2022.
- [68] L. Bottou, F. E. Curtis, and J. Nocedal, "Optimization methods for large-scale machine learning," *SIAM review*, vol. 60, no. 2, pp. 223–311, 2018.
- [69] H. Wang, J. Wang, and G. Wang, "Clustering validity function fusion method of fcm clustering algorithm based on dempster–shafer evidence theory," *International Journal of Fuzzy Systems*, vol. 24, p. 650–675, 2022.
- [70] J. Liu, X. Liu, Y. Yang, L. Liu, S. Wang, W. Liang, and J. Shi, "One-pass multi-view clustering for large-scale data," in *Proceedings of the IEEE/CVF International Conference on Computer Vision*, 2021, pp. 12 344–12 353.
- [71] X. Liu, L. Liu, Q. Liao, S. Wang, Y. Zhang, W. Tu, C. Tang, J. Liu, and E. Zhu, "One pass late fusion multi-view clustering," in *International Conference on Machine Learning*. PMLR, 2021, pp. 6850–6859.
- [72] H. Tao, C. Hou, X. Liu, T. Liu, D. Yi, and J. Zhu, "Reliable multi-view clustering," in *Proceedings of the AAAI conference on artificial intelligence*, vol. 32, no. 1, 2018.
- [73] H. Tang and Y. Liu, "Deep safe multi-view clustering: Reducing the risk of clustering performance degradation caused by view increase," in *Proceedings of the IEEE/CVF Conference on Computer Vision and Pattern Recognition*, 2022, pp. 202–211.
- [74] X. Wan, X. Liu, J. Liu, S. Wang, Y. Wen, W. Liang, E. Zhu, Z. Liu, and L. Zhou, "Auto-weighted multi-view clustering for large-scale data," in *Proceedings of the AAAI Conference on Artificial Intelligence*, vol. 37, no. 8, 2023, pp. 10 078–10 086.
- [75] C. Tang, Z. Li, J. Wang, X. Liu, W. Zhang, and E. Zhu, "Unified one-step multi-view spectral clustering," *IEEE Transactions on Knowledge and Data Engineering*, vol. 35, no. 6, pp. 6449–6460, 2023.
- [76] Z. Liu, H. Huang, S. Letchmunan, and M. Deveci, "Adaptive weighted multi-view evidential clustering with feature preference," *Knowledge-Based Systems*, vol. 294, p. 111770, 2024.
- [77] J. Chen, H. Mao, W. L. Woo, and X. Peng, "Deep multiview clustering by contrasting cluster assignments," in *Proceedings of the IEEE/CVF international conference on computer vision*, 2023, pp. 16 752–16 761.
- [78] M. Hu and S. Chen, "Doubly aligned incomplete multi-view clustering," in *Twenty-Seventh International Joint Conference on Artificial Intelligence IJCAI-18*, 2018.
- [79] J. Wen, Z. Zhang, Y. Xu, B. Zhang, L. Fei, and H. Liu, "Unified embedding alignment with missing views inferring for incomplete multi-view clustering," in *Proceedings of the AAAI conference on artificial intelligence*, vol. 33, no. 1, 2019, pp. 5393–5400.
- [80] J. Wen, Y. Xu, and H. Liu, "Incomplete multiview spectral clustering with adaptive graph learning," *IEEE Transactions on Cybernetics*, vol. 50, no. 4, pp. 1418–1429, 2020.
- [81] W. Shao, L. He, C. Lu, and P. S. Yu, "Online multi-view clustering with incomplete views," in *2016 IEEE International Conference on Big Data (Big Data)*, 2016, pp. 1012–1017.
- [82] M. Hu and S. Chen, "One-pass incomplete multi-view clustering," *Proceedings of the AAAI Conference on Artificial Intelligence*, vol. 33, pp. 3838–3845, 2019.
- [83] X. Wan, B. Xiao, X. Liu, J. Liu, W. Liang, and E. Zhu, "Fast continual multi-view clustering with incomplete views," *IEEE Transactions on Image Processing*, vol. 33, pp. 2995–3008, 2024.
- [84] Z. Yang, H. Zhang, Y. Wei, Z. Wang, F. Nie, and D. Hu, "Geometric-inspired graph-based incomplete multi-view clustering," *Pattern Recognition*, vol. 147, p. 110082, 2024.
- [85] G. Chao, Y. Jiang, and D. Chu, "Incomplete contrastive multi-view clustering with high-confidence guiding," in *Proceedings of the AAAI conference on artificial intelligence*, vol. 38, no. 10, 2024, pp. 11 221–11 229.
- [86] Z. Shi and H. Zhao, "Deep multi-view clustering based on reconstructed self-expressive matrix," *Applied Sciences*, vol. 13, no. 15, p. 8791, 2023.
- [87] X. Chen, Y. Han, C. Li, X. Chang, Y. Sun, and Y. Yang, "A static–dynamic composition framework for efficient action recognition," *IEEE Transactions on Neural Networks and Learning Systems*, pp. 1–14, 2025.
- [88] H. Zhong, H. Zhang, and F. Jia, "Analysis and improvement of evaluation indexes for clustering results," *EAI Endorsed Trans. Collab. Comput.*, vol. 4, no. 13, p. e4, 2020.